GEOPHYSICAL RESEARCH LETTERS, VOL. 33, L19819, doi:10.1029/2006GL026921, 2006

Offshore transport episodes of anthropogenic sulfur in northern Chile: Potential impact on the stratocumulus cloud deck

N. Huneeus,[1] L. Gallardo,[2] and J. A. Rutllant[3]

Received 16 May 2006; revised 24 July 2006; accepted 30 August 2006; published 13 October 2006.

[1] An outstanding meteorological feature appearing off the coast in Central and Northern Chile is the persistent stratus cloud deck under the subtropical Pacific High. It has a large impact on the regional and global energy balance and atmospheric circulation. In connection with mid-latitude synoptic-scale disturbances, subsiding easterly flow down the subtropical Andes often occurs in Northern Chile allowing large anthropogenic emissions of oxidized sulfur that take place in the region to reach the stratus deck. We explore the potential impact of anthropogenic emitted sulfur on the stratus deck associated with strong easterly flow events that occur on the average 4 to 8 times per year. A representative transport event is simulated using a 3-D transport chemistry model and the results are compared with satellite observations of cloud droplet number concentration. Although not conclusive, this preliminary study reveals a potential perturbation of the subtropical stratocumulus deck due to anthropogenic sulfur aerosols. **Citation:** Huneeus, N., L. Gallardo, and J. A. Rutllant (2006), Offshore transport episodes of anthropogenic sulfur in northern Chile: Potential impact on the stratocumulus cloud deck, *Geophys. Res. Lett.*, *33*, L19819, doi:10.1029/2006GL026921.

1. Introduction

[2] The world's most extended and persistent stratus deck is that located under the subtropical Pacific High off the coast of Northern Chile and Southern Peru. This cloud deck has a large impact on the regional and global atmospheric circulations [e.g., *Hartmann et al.*, 1992]. In this region large emissions of oxidized sulfur (SO_x = sulfur dioxide (SO_2) + sulfate (SO_4)) occur, both due to anthropogenic processes [e.g., *Lefhon et al.*, 1999], mainly copper smelting, and natural processes as biogenic emissions along the Humboldt Current system [e.g., *Boucher et al.*, 2003], and volcanic emissions [e.g., *Anders and Kasgnoc*, 1998; *Mather et al.*, 2004]. Whereas anthropogenic emissions are relatively well constrained (±20–30%), natural emissions are very uncertain as this region is largely void in terms of biogeochemical observations and monitoring [e.g., *Earth Observing Laboratory*, 2006].

[3] On the synoptic scale, it has been shown that migratory highs drifting eastwards across Southern Chile ahead of mid-troposphere ridges induce subsiding easterly flow off Central Chile [*Garreaud et al.*, 2002] that cause coastal low-cloud clearings, enhanced upwelling-favorable winds and the subsequent poleward propagation of atmospheric coastally-trapped disturbances. These conditions are crucial for determining potential fluxes of biogenic sulfur [e.g., *Hormazábal et al.*, 2001], increased pollution potentials and offshore dispersion of pollutants, particularly anthropogenic sulfur [e.g., *Gallardo et al.*, 2002].

[4] Here we explore the plausibility of a potential anthropogenic perturbation in the stratocumulus (Sc) deck off Northern Chile due to transport of sulfur emissions from copper smelting in connection with easterly wind events. This is particularly relevant within the framework of upcoming research dealing with aerosol-cloud-drizzle interactions in the Southeast Pacific [*Earth Observing Laboratory*, 2006, and references therein]. This is done by performing simulations with a chemistry-transport-deposition model under strong easterly wind conditions. The dispersion pattern of sulfur emissions is then compared with cloud droplet number concentration (CDNC) fields derived from satellite observations. In the next section we describe the data and methodology used for the analysis. Results, including synoptic weather pattern composites, simulations of transport events and comparison with satellite products, are presented in Section 3. Preliminary conclusions are drawn in Section 4.

2. Data and Methodology

[5] Various data sources are considered in this study, namely rawinsonde data collected daily by the Chilean Weather Service at Cerro Moreno (23.43°S, 70.43°W, 137 m.a.s.l.), reanalysis and dynamically interpolated meteorological fields, and sulfur emissions from copper smelters. These data are used to characterize the synoptic scale circulation features and their frequency of occurrence in connection with offshore transport events, and to feed a dispersion model. The dispersion patterns obtained through model simulations are compared with horizontal cloud droplet number concentration. A brief summary of the data and their application follows.

2.1. Sounding Data and Offshore Wind Events

[6] The data used to define easterly transport events come from daily rawinsoundings (12 UTC; 8:00 AM local time) at Antofagasta, Cerro Moreno (23.43°S, 70.43°W, 137 m.a.s.l.) obtained from the University of Wyoming web site (http://www.weather.uwyo.edu/upper air). These data cover the period between January 1, 1989 and December 31, 2002, i.e., a total of 14 years that include both warm (El Niño) as well as cold (La Niña) phases of the El Niño-Southern Oscillation (ENSO) cycle. Since the focus of

[1]Laboratoire d'Optique Atmosphérique, CNRS UMR 8518, Université des Sciences et Technologies de Lille, Villenueve d'Ascq, France.
[2]Center for Mathematical Modeling, University of Chile, CNRS UMI 2807, Casilla, Santiago, Chile.
[3]Department of Geophysics, University of Chile, Santiago, Chile.

0094-8276/06/2006GL026921$05.00

Table 1. Emissions and Deposition Parameters Used in the Dispersion Simulation

Parameter\Species	Emissions, GgS/yr SO_2_S	SO_4_S
Smelters		
Chuquicamata (22.32S, 68.92 W, 2850 m.a.s.l.)	100,7	5,3
Potrerillos (26.43S, 69.47W, 2850 m.a.s.l.)	40,9	2,2
Noranda (23.98S, 70.07 W, 1272 m.a.s.l)	19,0	1,0
Paipote (27.42S, 70.25 W, 540 m.a.s.l.)	12,4	0,7
Power plants		
Tocopilla (22.08°S, 70.4°W, 50 m.a.s.l.)	31,4	1,7
Huasco (28.5°S, 71, 32°W, 25 m.a.s.l.)	14,3	0,8
Dry deposition		
Over land (min/max), cm/s	0,3/0,8	0,1/0,1
Over water in cm/s	0,5	0,05
Wet deposition, s − 1·/(mm · hour − 1)	$0{,}69 \times 10^{-4}$	$2{,}78 \times 10^{-4}$

the study is offshore transport, events were defined solely based on the zonal wind component. Further, since the largest anthropogenic sulfur emissions (Table 1) take place in copper smelting plants located at about 3 km altitude, we defined "strong easterly wind events" as those when the easterly wind component at Antofagasta exceed 5 m/s at 700 hPa. This is a relatively strict criterion since the largest seasonal average of the easterly wind component for this location is 2.3 m/s in winter, when easterly winds peak in intensity.

2.2. Reanalysis Data and Synoptic Weather Conditions

[7] The large-scale tropospheric circulation pattern for each easterly wind event (as defined in the previous section) was characterized using ERA-40 reanalysis fields [e.g., *Simmons and Gibson*, 2000]. These fields have a horizontal resolution of about 1° or about 125 km in the horizontal and 60 levels in the vertical from the surface up to about 65 km altitude.

2.3. Emissions

[8] We considered the emissions from four copper smelters located in Northern Chile, namely: Chuquicamata, Potrerillos, Noranda, and Paipote [*National Commission for the Environment*, 2001]. These are by far the dominant anthropogenic sources of oxidized sulfur in the area. In addition to this, we considered upper limit emission estimates for the Tocopilla and Huasco power plants located by the coast in Northern Chile. No urban emissions were considered since according to previous estimates these are negligible compared with other anthropogenic sources in this area [*Huneeus*, 2003]. The emission data are summarized in Table 1.

2.4. High-Resolution Weather Data

[9] The data used to drive the transport model correspond to high resolution (0.1° ∼ 11 km) meteorological data derived from a dynamical interpolation of global analyses from the European Center for Medium Range Weather Forecast (ECMWF) down to a 0.1° horizontal resolution, every 3 hours, which are available from previous work. These fields have been extensively evaluated against data collected at synoptic stations as well as at a dense meteorological network in the Metropolitan area of Santiago (33.5°S, 70.8°W, 500 m.a.s.l.), including a sounding station in the outskirts of Santiago [*Gallardo et al.*, 2002]. All in all, these fields capture the regional scale circulation patterns, including synoptic variations (moving low- and high-pressure systems and fronts). Radiatively driven circulations such as those that develop at the slopes of the Andes Cordillera are well described in these fields, particularly over Northern Chile [*Huneeus*, 2003]. However the depth of the marine boundary layer (MBL), and hence the Sc layer top, is too shallow when compared with observations. These errors have been known for a decade [e.g., *Mechoso et al.*, 1995], and are common to current meteorological models used in operational weather forecasting. Better results can be achieved using higher vertical resolutions and more sophisticated parameterization schemes within the MBL [e.g., *Garreaud and Muñoz*, 2005].

2.5. Cloud Droplet Number Concentration (CDNC)

[10] The Earth Observing System (EOS) facility provides, through the Moderate Resolution Imaging Spectroradiometer (MODIS), world-wide monitoring of several atmospheric properties, including optical depth, liquid water path and effective cloud droplet radius at 1 km resolution [e.g., *King et al.*, 2003; *Platnick et al.*, 2003]. These retrievals rely on radiative transfer models and assumed particle size distributions. Furthermore, the retrieval algorithms assume a single-layer, liquid water, and plane-parallel geometry. Also, errors are expected to occur when ice clouds are present. The former assumption appears adequate for the Sc deck but the latter may suggest interference due to the presence of cirrus clouds, which are frequently present over this region. We consider here the available data for the so-called level two MODIS cloud products, i.e., effective particle radius (r_{eff}), cloud top pressure, liquid water path (LWP) and cloud cover for the period July 20–August 20, 2000. These data were downloaded from the MODIS atmosphere web site (http://modis-atmos.gsfc.nasa.gov/MOD06_L2/index.html). The CDNC was calculated according to:

$$CDNC \approx \frac{3LWP}{4\pi\rho_w k H r_{eff}^3}$$

where H is the cloud thickness, ρ_w the density of water and k a constant [*Martin et al.*, 1994]. We assume H ∼ 0.5 km, $k = 0.8$ and $\rho_w = 1.0 \times 10^3$ Kg/m^3.

3. Results

3.1. Synoptic Conditions and Transport Patterns

[11] "Strong easterly wind days" (SEDs), i.e., speeds in excess of 5 m/s at 700 hPa, tend to be evenly distributed in

all seasons with a slight preference for fall, with 4 to 8 SEDs per year. No discernible bias towards either extreme of the ENSO cycle appears, except for the strong La Niña in 1999 when 14 SEDs, of a total of 82 in the 14 year period, occurred. Consecutive SEDs were grouped into strong easterly events (SEEs) yielding 74 SEEs during this period.

[12] SEDs happen in connection with ridging in the mid-troposphere with the ridge axis just west of the study area (S-SW winds aloft), as depicted in 500 hPa geopotential height and sea-level pressure (SLP) composites (Figure 1a). The onset of anomalous easterlies is preceded one day by anomalous warming between 850 and 900 hPa and anomalous drying above (not shown). These circulation conditions present a synoptic structure typical of the coastal troughing at the onset stage of coastal-low events farther south in Chile [e.g., *Garreaud et al.*, 2002].

[13] As an example of a typical SED, a case study for July 26, 2000 is presented in the next section. The representativeness of this case is documented by the actual 500 hPa geopotentials and SLP fields (Figure 1b), featuring a typical mid-troposphere ridge axis tilted in a NW-SE direction over Northern Chile and a surface trough between the subtropical anticyclone to the west and a migratory high east of the Andes.

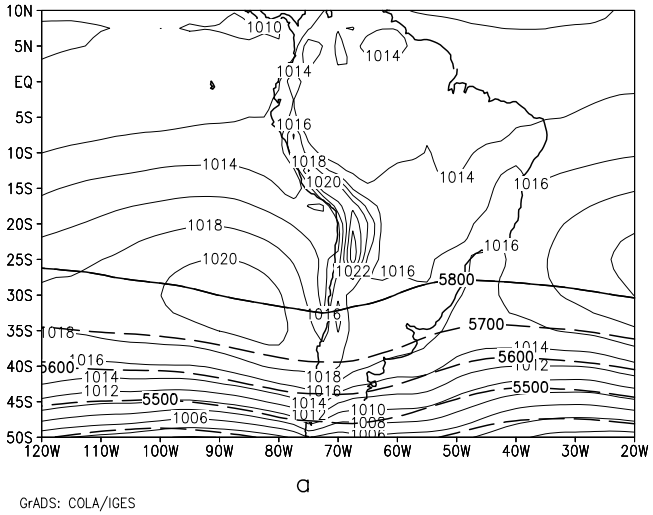

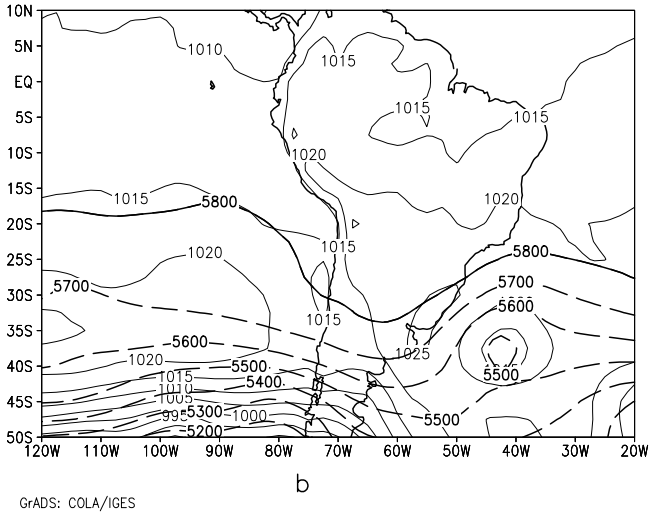

Figure 1. (a) Composited surface pressure (thin lines) and 500 hPa geopotential contours (thick lines), considering 82 days of strong easterly winds at Antofagasta (23°S). (b) Corresponding configuration for July 26th, 2000.

3.2. Dispersion Simulations

[14] To illustrate the effects of the synoptic conditions identified above (2.1.), we performed a numerical simulation using a transport/chemistry/deposition off-line model, the Multi-scale Atmospheric Transport and Chemistry model (MATCH, [*Robertson et al.*, 1999]). We used a similar model set-up as in previous work [e.g., *Gallardo et al.*, 2002], except that the domain now spanned from 30°S to 20°S and from 67°W to 75.45°W, and from the surface up to approximately 7 km height (i.e., 16 hybrid model layers). The emissions used and the deposition parameters chosen are shown in Table 1. A one month-long simulation was conducted for a winter period between July 20 and August 19 2000. This period was chosen based on the availability of MODIS data.

[15] Close to the sources and over land SO_2 is, as expected, the prevailing form of oxidized sulfur, adding up to 80% of the total sulfur budget (not shown). On average, this fraction decreases offshore where the partitioning is more evenly distributed between SO_2 and SO_4. This reflects the effects of oxidation processes and the lack of inputs of fresh SO_x by in situ sources.

[16] Within the one-month period in which MODIS data were available, the SEE centered on July 26th was selected as a representative case (Cf. Figure 1). When transported offshore on around July 26th 2000, most of the SO_x remains confined between the top of the Sc layer and up to 4 km above the surface (Cf. Figure 2). In this layer, SO_x mixing ratios increase in one order of magnitude compared with the average condition. The SO_2 transported offshore right above the MBL is efficiently incorporated into the Sc layer and subsequently oxidized to sulfate and wet deposited. These features are illustrated in Figure 2, where the vertical and horizontal distributions of oxidized sulfur are shown.

3.3. Satellite Data

[17] In Figure 3, we compare CDNC between the day of the easterly wind event, i.e., July 26th, and the average for the period July 20–August 20 2000. A clear increase in CDNC is observed downwind from the SO_x sources, in a very similar pattern to that of oxidized sulfur during July 26th, suggesting an anthropogenic impact. An area with persistently high CDNC is noticed along the coast and offshore between 30°S and 26°S, which is not readily associated with anthropogenic sulfur emissions. We speculate that this feature could be explained by coastal upwelling-related biogenic emissions driven by strong southerlies in this region [e.g., *Garreaud and Muñoz*, 2005] or dust emissions from the semi-arid areas of Central Chile.

[18] Relating CDNC and aerosol concentrations is not straightforward. Nevertheless, several relationships have been found in field and mechanistic studies [e.g., *Penner et al.*, 2001]. For example, *Leaitch et al.* [1992], based on hundred of simultaneous measurements of CDNC (cm^{-3}) and sulfate concentrations ($\mu g/m^3$), found for stratiform clouds:

$$\log(CDNC) = (0.257 \pm 0.052) * \log(SO4) + 1.95 \pm 0.21$$

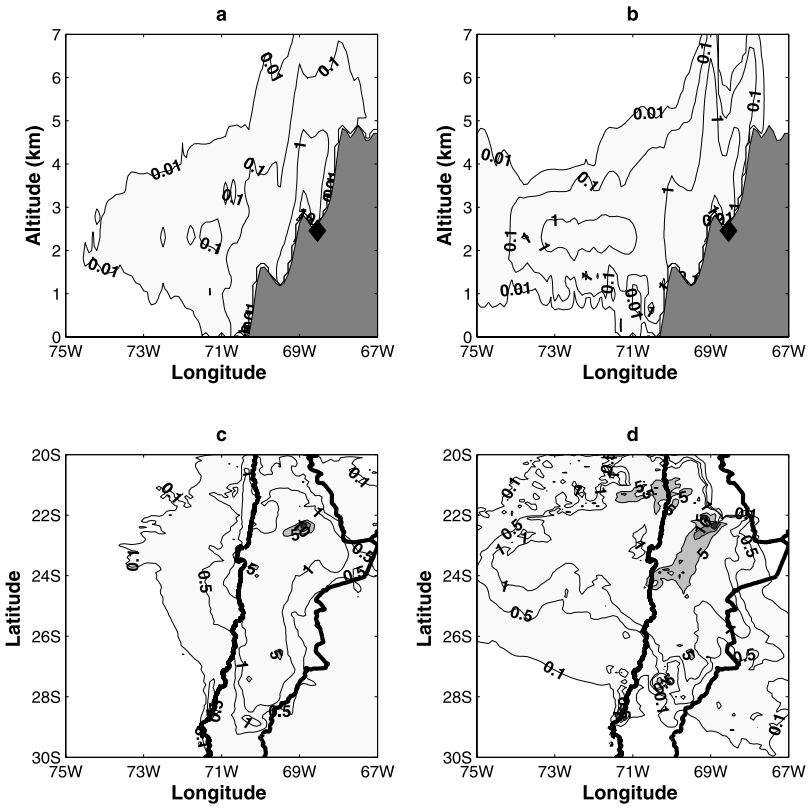

Figure 2. (a and b) Cross-sections at latitude 23.3°S of mass mixing ratios of SO_x (in ppbm). To the left the monthly averaged distribution and to the right daily averages for July 26th are shown. (c and d) Burden, i.e., vertically integrated mass of SO_x (in mgS/m^2).

Adopting this approach, a one order of magnitude change in oxidized sulfur, in connection with easterly wind events as those simulated here, should result in 1.6 to 2 fold increase in CDNC, which is actually observed (Figure 4).

4. Concluding Remarks

[19] This study has explored the potential perturbation of the subtropical Sc deck off Northern Chile by anthropogenic sulfur emissions (copper smelters) in connection with strong

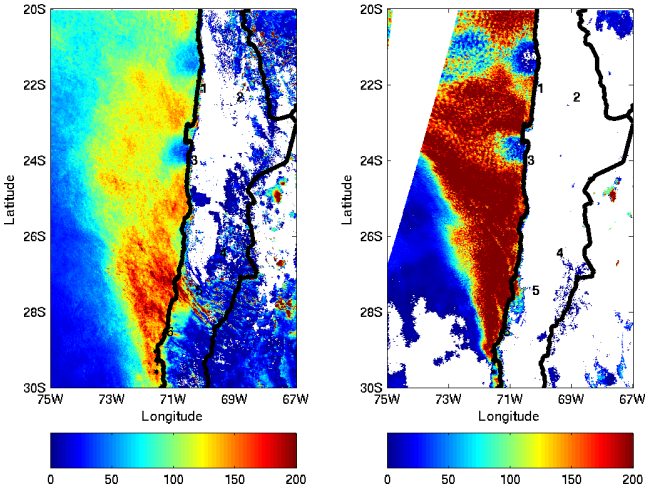

Figure 3. Cloud droplet number concentration (CDNC, in cm^{-3}). (left) Average CDNC for the period between July 20 and August 20, 2000. (right) CDNC for July 26th in connection with the easterly wind event. Displayed on the figure are the location of the power plant Tocopilla (1) and cooper smelters Chuquicamata (2), Noranda (3), Potrerillos (4) and Paipote (5).

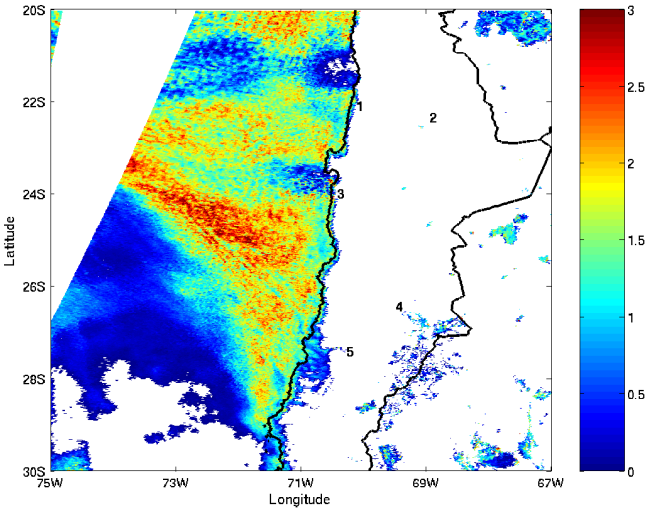

Figure 4. Ratio of cloud droplet number concentration (CDNC, cm^{-3}) between July 26th and the average CDNC for the period July 20 and August 20 2000 (Cf. Figure 1). Displayed on the figure are the location of the power plant Tocopilla (1) and cooper smelters Chuquicamata (2), Noranda (3), Potrerillos (4) and Paipote (5).

easterly wind events (>5 m/s at 700 hPa). For a 14 year period (1989–2002) 74 events, evenly distributed in all seasons with a slight preference for fall, could be identified. Days with strong easterly wind present a synoptic structure typical of the coastal troughing at the onset stage of coastal-low events farther south in Chile: ridging in the middle troposphere providing for a weakening of the westerlies (allowing even easterlies), a downslope flow in the western Andes and a consequent strengthening and descent of the coastal subsidence inversion base [e.g., *Garreaud et al.*, 2002]. Given the high threshold for the easterly wind anomaly used in the definition of SEDs, easterly wind events appear to be quite common, reflecting the potential importance for the stratocumulus cloud deck in modifying their optical characteristics and hence their role in the regional radiation budget.

[20] Simulations performed with a 3-D emission-transport-deposition model of an easterly wind event around July 26th 2000 show that, consequently with the synoptic configuration described above, the SO_x emitted from copper smelters located over the western slope of the Andes is transported offshore, remaining mostly within the layer between the top of the Sc and 4 km above the surface. Concomitantly, an increase in CDNC can be appreciated downwind of the main emission sources. Assuming a log-log relationship between sulfate concentration and CDNC, the observed changes in CDNC are consistent both in pattern and in magnitude with the changes due to the offshore transport of oxidized sulfur, suggesting a potential anthropogenic impact on the stratus deck. Although suggestive, these data and simulations do not prove nor quantify an anthropogenic perturbation of the optical properties in the Sc deck off the Chilean coast. Other factors might also explain the observed changes in CDNC. For instance, biogenically produced aerosols, not only sulfur aerosols, may also induce changes, particularly considering that easterly wind events are generally associated with near surface southerlies along the coast enhancing upwelling and air-sea gas exchange [e.g., *Rutllant et al.*, 2003]. Hence, in order to ascertain the validity of our hypothesis further research must be conducted. Such research should consider in situ measurements and characterization of active cloud condensation nuclei in the Sc deck and air-borne particles that may become activated. Also, efforts should be made to quantify biogenic fluxes and air-sea exchange in general, including the effects of dust and iron deposition. Such data in combination with process-oriented cloud models and regional atmospheric circulation models may provide a solid basis for quantifying the effects of anthropogenic and natural aerosols on the Sc deck off the Chilean coast.

[21] **Acknowledgments.** This work has been developed within the framework of ECOS Sud collaboration agreement (C03U04), and under research grants FONDECYT 1020833 and PRODAC (Universidad de Chile). Discussions and comments from Annica Ekman and Jerome Riedi are greatly appreciated. We are also grateful for the assistance of M.Sc. D. Painemal, and the constructive comments provided by two anonymous reviewers.

References

Anders, R. J., and A. D. Kasgnoc (1998), A time averaged inventory of subaerial vulcanic sulfur emissions, *J. Geophys. Res.*, *103*, 25,251–25,261.

Boucher, O., et al. (2003), DMS atmospheric concentrations and sulphate aerosol indirect radiative forcing: A sensitivity study to the DMS source representation and oxidation, *Atmos. Chem. Phys.*, *3*, 9–65.

Earth Observing Laboratory (2006), VAMOS Ocean-Cloud-Atmosphere-Land Study (VOCALS), VOCALS-Southeast Pacific Regional Experiment (REx), Natl. Cent. for Atmos. Res., Boulder, Colo. (Available at http://www.joss.ucar.edu/)

Gallardo, L., G. Olivares, J. Langner, and B. Aarhus (2002), Coastal lows and sulfur air pollution in Central Chile, *Atmos. Environ.*, *36*(23), 3829–3841.

Garreaud, R., and R. Muñoz (2005), The low-level jet off the subtropical coast of South America: Structure and variability, *Mon. Weather Rev.*, *133*, 2246–2261.

Garreaud, R., J. Rutllant, and H. Fuenzalida (2002), Coastal lows along the subtropical west coast of South America: Mean structure and evolution, *Mon. Weather Rev.*, *130*, 75–88.

Hartmann, D., M. Ockert-Bell, and M. Michelsen (1992), The effect of cloud type on Earth's energy balance: Global analysis, *J. Clim.*, *5*, 1281–1304.

Hormazábal, S., G. Shaffer, J. Letelier, and O. Ulloa (2001), Local and remote forcing of sea surface temperature in the coastal upwelling system off Chile, *J. Geophys. Res.*, *106*, 16,657–16,672.

Huneeus, N. (2003), Dispersión de azufre oxidado en el norte de Chile, M.Sc. Atmospheric Sciences, Geophys. Dep., Univ. of Chile, Santiago, Chile.

King, M. D., W. P. Menzel, Y. J. Kaufman, D. Tanre, B.-C. Gao, S. Platnick, S. A. Ackerman, L. A. Remer, R. Pincus, and P. A. Hubanks (2003), Cloud and aerosol properties, precipitable water, and profiles of temperature and water vapor from MODIS, *IEEE Trans. Geosci. Remote Sens.*, *41*, 442–458.

Leaitch, W. R., G. A. Isaac, J. W. Strapp, C. M. Banic, and H. A. Wiebe (1992), The relationship between cloud droplet number concentrations and anthropogenic pollution: Observations and climatic implications, *J. Geophys. Res.*, *97*(D2), 2463–2474.

Lefhon, A. S., J. D. Husar, and R. B. Husar (1999), Estimating historical anthropogenic global sulfur emission patterns for the period 1850–1990, *Atmos. Environ.*, *33*(21), 3435–3444.

Martin, G. M., D. W. Johnson, and A. Spice (1994), The measurement and parametrization of effective radius of droplets in warm stratocumulus clouds, *J. Atmos. Sci.*, *51*, 1823–1842.

Mather, T. A., V. I. Tsanev, D. M. Pyle, A. J. S. McGonigle, C. Oppenheimer, and A. G. Allen (2004), Characterization and evolution of tropospheric plumes from Lascar and Villarrica volcanoes, Chile, *J. Geophys. Res.*, *109*, D21303, doi:10.1029/2004JD004934.

Mechoso, C. R., et al. (1995), The seasonal cycle over the tropical Pacific in general circulation models, *Mon. Weather Rev.*, *123*, 2825–2838.

National Commission for the Environment (2001), Antecedentes para la Revisión de las Normas de Calidad de Aire Contenidas en la Resolución N° 1215 del Ministerio de Salud (in Spanish), Santiago, Chile. (Available at http://www.conama.cl)

Penner, J. E., et al. (2001), Aerosols, their direct and indirect effects, in *Climate Change 2001: The Scientific Basis*, edited by J. T. Houghton et al., chap. 5, pp. 289–416, Cambridge Univ. Press, New York.

Platnick, S., M. D. King, S. A. Ackerman, W. P. Menzel, B. A. Baum, J. C. Riédi, and R. A. Frey (2003), The MODIS cloud products: Algorithms and examples from Terra, *IEEE Trans. Geosci. Remote Sens.*, *41*, 459–473.

Robertson, L., J. Langner, and M. Engardt (1999), An Eulerian limited-area atmospheric transport model, *J. Appl. Meteorol.*, *38*, 190–210.

Rutllant, J., H. Fuenzalida, and P. Aceituno (2003), Climate dynamics along the arid northern coast of Chile: The 1997–1998 Dinámica del Clima de la Región de Antofagasta (DICLIMA) experiment, *J. Geophys. Res.*, *108*(D17), 4538, doi:10.1029/2002JD003357.

Simmons, A. J., and J. K. Gibson (2000), The ERA-40 project plan, *ERA-40 Proj. Rep. Ser. 1*, 63 pp., Eur. Cent. for Med.-Range Weather Forecasts, Reading, UK. (Available at http://www.ecmwf.int/publications/)

L. Gallardo, Center for Mathematical Modeling, University of Chile, CNRS UMI 2807, Casilla 170-3, Santiago, Chile.

N. Huneeus, Laboratoire d'Optique Atmosphérique, CNRS UMR 8518, Université des Sciences et Technologies de Lille, F-59655 Villenueve d'Ascq, France. (huneeus@loa630.univ-lille1.fr)

J. A. Rutllant, Department of Geophysics, University of Chile, Casilla 2777, Santiago, Chile.